

Spatial Variation and Trend of Extreme Precipitation in Africa during 1981-2019 and Its Projected Changes at the End of 21st Century

Fabien Habiyakare^{1,2*}, Tong Jiang^{3#}, Ibrahim Yahaya^{1,4}, Daudi Ndabagenga¹, James Kagabo^{1,2}, Buda Su^{3#}

¹School of Atmospheric Sciences, Key Laboratory of Meteorological Disaster of Ministry of Education, Collaborative Innovation, Center on Forecast and Evaluation of Meteorological Disasters, Nanjing University of Information Science and Technology, Nanjing, China

²Rwanda Meteorology Agency (Meteo Rwanda), Kigali, Rwanda

³Institute for Disaster Risk Management/School of Geographical Sciences, Nanjing University of Information Science & Technology, Nanjing, China

⁴Department of Geography, Gombe State University, Gombe State, Nigeria
Email: fabineza1@gmail.com, [#]jiangtong@nuist.edu.cn, [#]subd@nuist.edu.cn

How to cite this paper: Habiyakare, F., Jiang, T., Yahaya, I., Ndabagenga, D., Kagabo, J., & Su, B. (2024). Spatial Variation and Trend of Extreme Precipitation in Africa during 1981-2019 and Its Projected Changes at the End of 21st Century. *Journal of Geoscience and Environment Protection*, 12, 192-221.

<https://doi.org/10.4236/gep.2024.123012>

Received: February 22, 2024

Accepted: March 26, 2024

Published: March 29, 2024

Copyright © 2024 by author(s) and Scientific Research Publishing Inc. This work is licensed under the Creative Commons Attribution International License (CC BY 4.0).

<http://creativecommons.org/licenses/by/4.0/>



Open Access

Abstract

This study comprehensively examines the patterns and regional variation of severe rainfall across the African continent, employing a suite of eight extreme precipitation indices. The analysis extends to the assessment of projected changes in precipitation extremes using five General Circulation Models (GCMs) from Coupled Model Intercomparison Project Phase 6 (CMIP6) under four Shared Socioeconomic Pathways (SSPs) scenarios at the long-term period (2081-2100) of the 21st century. Furthermore, the study investigates potential mechanisms influencing precipitation extremes by correlating extreme precipitation indices with oceanic system indices, specifically Niño 3.4 for El Niño-Southern Oscillation (ENSO) and Dipole Mode Index (DMI) for the Indian Ocean Dipole (IOD). The findings revealed distinct spatial distributions in mean trends of extreme precipitation indices, indicating a tendency toward decreased extreme precipitation in North Africa, Sahel region, Central Africa and the Western part of South Africa. Conversely, West Africa, East Africa and the Eastern part of South Africa exhibit an inclination toward increased extreme precipitation. The changes in precipitation extreme indices indicate a general rise in both the severity and occurrence of extreme precipitation events under all scenarios by the end of the 21st century. Notably, our analysis projects a decrease in consecutive wet days (CWD) in the far-future.

*First Author.

#Corresponding Author.

Additionally, correlation analysis highlights significant correlation between above or below threshold rainfall fluctuation in East Africa and South Africa with oceanic systems, particularly ENSO and the IOD. Central Africa abnormal precipitation variability is also linked to ENSO with a significant negative correlation. These insights contribute valuable information for understanding and projecting the dynamics of precipitation extreme in Africa, providing a foundation for climate adaptation and mitigation efforts in the region.

Keywords

Extreme Precipitation, Mann-Kendall Trend, Projections, Oceanic System, Africa

1. Introduction

Since the middle of 19th century, a surge in greenhouse gas concentration has resulted in a warming planet, causing elevated sea levels, reduced snow and ice coverage and significant alterations in global climate extremes regarding trends, frequency and intensity (Brohan et al., 2006; IPCC Working Group I et al., 2013; Schleussner et al., 2016). These extremes encompass unprecedented precipitation patterns that are neither uniformly distributed temporally nor spatially (Donat et al., 2013). Consequently, these changes have a deep effect on natural ecosystems, water management and agriculture, particularly in less-developed countries (Ge et al., 2021; Nikulin et al., 2018; Ogwang et al., 2015; Onyutha, 2018). In Africa, the majority of the population relies on farming for subsistence, as highlighted by the International Water Management Institute (IWMI) in 2014. Precipitation is the climatic factor with the greatest impact; its excessive (rarity) occurrences cause flooding (droughts) which are frequently accompanied by a lack of food and energy, the loss of life and properties and other social-economic disruptions (Indeje & Semazzi, 2000; Ogwang et al., 2015; Onyutha, 2018).

A number of studies have been exploring features of increased intensity of extreme rainfall, a rapid variability of dry spell lengths and wet spell lengths have shown subsequent reaction of climatic variability over the study area (Almazroui et al., 2020; Ayugi et al., 2021; Giorgi, Raffaele, & Coppola, 2019). Past studies have confirmed the decrease in annual precipitation over Africa (Marra, Leviziani, & Cattani, 2022; Onyutha, 2017, 2018; Tierney, Ummenhofer, & Peter, 2015) while the projected outlook from other studies and reports indicates an expected increase in area-averaged precipitation across Africa (Donat et al., 2013; IPCC Working Group I et al., 2013). The witnessed changes in annual and seasonal precipitation patterns in different regions are greatly believed to be caused by climate change, leading to shift in the timing, duration and geographic distribution of extreme precipitation events (IPCC, 2021; Roberts et al., 2022). Although natural factors like volcanic eruptions are said to cause climate change

(Aubry et al., 2022; Stenchikov, 2021), different researches confirm anthropogenic factors to be the main reason for the observed climate fluctuation. In this regard, industrial development contributes significantly to climate change through various processes that release greenhouse gases (GHGs) and other pollutants into the atmosphere (Syamsuri, Sulistyowati, & Wibawa, 2019; Wadnambi et al., 2020). Since the production of these aerosols accounts for climate change, a main factor for extreme precipitation variability, it is very crucial to account their effect in the analysis of trends in both historical period and future projection. In order to provide a framework for exploring a range of future scenarios and understanding how different socioeconomic pathways contribute to or mitigate the emissions of these greenhouse gases, this study employs climate models from the Climate Model Intercomparison Project (CMIP6) into consideration, involving four Shared Socioeconomic Pathways (SSPs) scenarios namely, SSP1-2.6 (sustainability), SSP2-4.5 (middle of the road), SSP 3 - 7.0 (regional rivalry) and SSP 5 - 8.5 (fossil-fueled development). Several studies (Almazroui et al., 2020; Danso et al., 2022; Dosio et al., 2021; Yahaya et al., 2024) employed the CMIP6 due to giving opportunities to increase our understanding of the effects of compounded global warming on climate change. Relevant stakeholders desperately need relevant evidence that will allow them to deal with pertinent difficulties such as those that pinpoint the precise patterns of historical changes, the degree of the shift and future projects (Ayugi et al., 2021).

In the context of climate change, gaining a more comprehensive understanding of the fluctuations in precipitation patterns offers valuable insights into water resource management and the prevention of floods and droughts (IPCC, 2022; Roberts et al., 2022). This is particularly crucial in Africa, where rain fed agriculture is prevalent. Similarly, the analysis of trends stands out as a primary method for forecasting forthcoming alterations in precipitation patterns. In recognizing robustness of examining climate variability, the Commission for Climatology (CCI) of the World Meteorological Organization (WMO), the Climate Variability and Predictability (CLIVAR) and the Joint WMO-IOC Technical Commission for Oceanography and Marine Meteorology (JCOMM) here after referred as Expert Team on Climate Change Detection and Indices (ETCCDI) has developed set of climatic indices, spanning from the stratosphere to the surface and subsurface ocean allowing the comparison between actual observations and simulated data (World Climate, 2007; Zhang et al., 2019; Zhang et al., 2011). Our study also used the same approach in the analysis. The reason for utilizing indices in this assessment is justified by their ability to represent crucial impact-relevant elements of the climate system, integrating information from various components.

Although different literature review have examined changes and frequency over different parts of the continent like (Ayugi et al., 2021) in East Africa, (Datta et al., 2020; Onyutha, 2018) over West Africa and (McBride, Kruger, & Dyson, 2022) in South Africa yet some regions remained untouched. Also (Almazroui et al., 2020) examined projected changes in temperature and precipitation

over Africa employing area average method while (Marra et al., 2022) investigated intensity in daily extreme precipitation over Africa using non-asymptotic statistical approach. The trends of some regions like Central Africa and Sahara need to be further explored. In order to address the existing gap in the literature, this research aims to examine frequency and intensity of trends of Extreme precipitation indices in the period (1981-2019) with their projection changes in far future (2081-2100) employing ETCDDI methodology (World Climate, 2007) over Africa continent using high-resolution Climate Hazards Group InfraRed Precipitation data with Station (CHIRPS). Also, it utilized CMIP6 model ensembles for projecting the future changes in precipitation extremes with SSPs scenarios for Africa over 21st century. In order to understand how the oceanic systems affect precipitation distribution in the tropics we extended our analysis in assessing oscillating warming and cooling pattern on extreme precipitation variability in the study area. The study of extreme precipitation trends plays a great role in water resource management, infrastructure planning and design as well as agriculture planning. Also, SSPs play a vital role in examining and comprehending potential scenarios for worldwide societal progress, especially concerning climate change. They offer a unified structure for analyzing scenarios, aiding in making well-informed decisions, formulating policies and fostering global cooperation to tackle the complexities of sustainable development and mitigating climate change (Kriegler, 2016).

2. Data and Methodology

2.1. Study Area

Africa's geographical coordinates span from Latitude 37°21'N to 34°51'15"S and Longitude 51°27'52"E to 17°33'22"W (see **Figure 1**). The continent encompasses a land area of roughly 30,365,000 square km, excluding nearby islands, extending approximately 8000 km from north to south and around 7400 km from east to west (Nwaerema, Edokpa, & Ajiere, 2019).

The average elevation of the continent's topography is approximately 600 meters above sea level. This elevation is more pronounced in the southern and eastern regions of Africa, contributing to cooler temperatures in comparison to other regions. The most significant climatic factors in Africa are rainfall and temperature. The Inter-Tropical Convergence Zone (ITCZ) operates between Latitudes 30° North and South of the Equator. It interacts with the Sub-tropical High Pressure Belts, which play a crucial role in shaping surface wind patterns and impacting the rainfall and temperature patterns across the continent (Barry & Chorley, n.d.).

2.2. Data

2.2.1. Observation Data

The study utilized the CHIRPS data version 2 (Funk et al., 2015), which covers the period 1981-2019 (39 years) with global land-only daily precipitation estimates at 0.25° × 0.25° resolution. The selected interval of time considers the suggested WMO reference climatological period covering more than 30 years

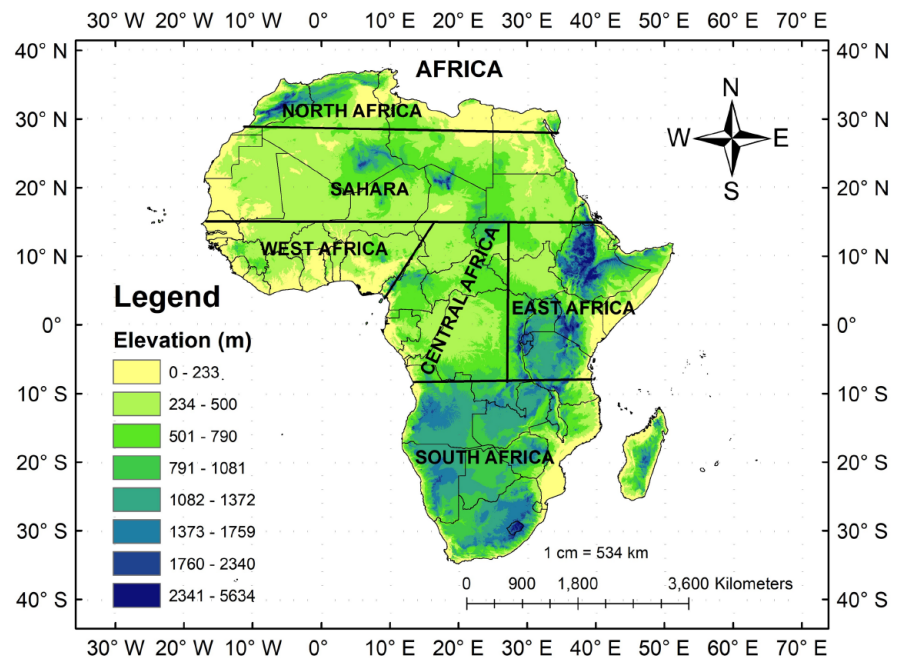


Figure 1. Study area.

(Climate Bulletin, 2021). The CHIRPS algorithm relies on precipitation estimates derived from the duration of cold cloud activity observed in infrared (IR) imagery captured by geostationary satellites. This algorithm also incorporates data from rain gauges through a merging procedure. The detailed information provided by high-resolution IR imagery is essential for accurately capturing the dynamics of short-lived local and mesoscale convective systems. These systems play a vital role in identifying extreme weather events, even at the daily scale (Raghavendra et al., 2018). CHIRPS is acknowledged as a benchmark for its robustness and high quality, particularly in Africa continent and is extensively employed in climatological investigations (Dembele, Schaeffli, & Van De Giesen, 2020). It is distinguished by its sufficiently high resolution and possesses extended, continuous, and consistent datasets, enabling the detection of trends across multiple scales over several decades.

Monthly SST data are the Extended Reconstructed SST V5 provided by the U.S. National Oceanic and Atmospheric Administration (NOAA) with a horizontal resolution of $2^\circ \times 2^\circ$ during 1981-2019 (Huang et al., 2017).

2.2.2. GCMs Dataset

The daily precipitation data retrieved from CMIP6 model ensembles were downloaded the fifth generation of the European Centre for Medium-Range Weather Forecasts (ECMWF) atmospheric reanalysis of the world climate (ERA5), spanning the years from January 1940 through the present (Hersbach et al., 2020). These data are available online through the following link: <https://cds.climate.copernicus.eu/cdsapp/dataset/projections-cmip6?tab=overview> (accessed: 20 August 2023) (refer Table 1) pertain to the initial realization (r1i1p1f1) from five models characterized by resolution of $(1^\circ \times 1^\circ)$ Projections regarding

Table 1. Summary of the five CMIP6 models used in this study.

No	Model	Model	No. of atmospheric grid points (lon. × lat.)
1	BCC-CSM2-MR	BCC-CMA/China	320 × 160
2	CanESM5	CCCMA/Canada	128 × 64
3	CNRM-CM6-1	CNRM-CERFACS/France	256 × 128
4	MRI-ESM2-0	MRI/Japan	192 × 96
5	IPSL-CM6A-LR	IPSL/France	144 × 143

changes of extreme precipitation in long term period were made under four scenarios known as SSPs. These SSPs were identified as SSP1-2.6 (sustainability), SSP2-4.5 (middle-of-the-road), SSP 3 - 7.0 (regional rivalry), and SSP 5 - 8.5 (fossil-fueled development). SSP2-4.5 is often characterized as a more moderate compared to some other pathways, suggesting that moderate mitigation efforts could limit global warming to approximately 2.5°C relative to the pre-industrial period by the end of the year 2100 (O'Neill et al., 2016). In contrast, SSP5-8.5, termed “business as usual,” depicts future characterized by fossil-fuel dependence, high challenges to both mitigation and adaptation efforts in climate change and a trajectory associated with significant global warming, potentially reaching around 5 degrees Celsius or more by the end of 21st century (O'Neill et al., 2016). This study utilized historical simulations covering the reference period of 1995-2014. For future projections, the analysis was conducted for the period of 2081-2100 (long-term period).

It's crucial to highlight that in this study, the models' output was utilized in their original states without applying post-processing or bias-correction techniques. This decision stems from the recognition that bias adjustment alone cannot address the inherent limitations of the models in accurately representing fundamental physical mechanisms. The reliability of the models' projections remains questionable Even after bias correction (Ayugi et al., 2021; Maraun et al., 2017). Datasets underwent remapping using a technique that re-gridded them to a grid (resolution) of (1° × 1°).

2.3. Methodology

2.3.1. Climate Indices

In this study, as endorsed by the ETCCDI, we calculated eight climate indices related to precipitation (World Climate, 2007; Sillmann et al., 2013; Zhang et al., 2011), these indices allow to assess the frequency, intensity, and duration of precipitation extreme events. Calculating indices by utilizing The RCLim-dex software package has followed standardized methodologies recommended by ETCCDI (World Climate, 2007; Project Team ECA&D, 2021) and approved by WMO. Here after computing indices, it becomes feasible to minimize climate fluctuations by merging various aspects of the climate system, enabling a comparison of their fluctuations. To be noticed, indices derived

from observational data, show greater consistency compared to those calculated from model outputs (World Climate, 2007). These indices are accessible at (<http://etccdi.pacificclimate.org/indices.shtml>) and displayed in **Table 2**.

The selection of extreme precipitation indices is also aimed at evaluating anticipated changes in the frequency, intensity, and duration of regional precipitation extremes. A recent investigation across various African regions (Akinsanola, Ongoma, & Kooperman, 2021) employed the mentioned indices to assess the ability of CMIP6 models in replicating the present features and spatial arrangement of extreme precipitation. Significant findings from the study affirmed the effectiveness of multi-model ensemble(MME) in depicting observed precipitation and associated extremes, surpassing individual model throughout the periods of rainfall (Ayugi et al., 2021).

2.3.2. Trend Analysis

The analysis of trends and variation in precipitation extreme events involves different statistical methods like linear regression analysis, Spearman test (SR), Sen's slope, Theil-Sen approach and Mann-Kendall test (MK) and among others. These statistical methods have been used by number of studies in examining precipitation trends analysis (Agarwal, Suchithra, & Gurjar, 2021; Fan et al., 2022; Ndabagenga et al., 2023). But this study opts MK method (Mann, 1945) in analysis due to its reliability non-parametric nature, MK is not influenced by the non-normality of the data. Additionally, it exhibits low sensitivity to abrupt breaks in inhomogeneous series (Agarwal et al., 2021). Good enough (MK) trend test (Mann, 1945) is recommended by WMO, along with the test of Sen. According to the null hypothesis H_0 , the data exhibits independence and a random distribution, whereas the alternative hypothesis H_1 suggests the existence of a monotonic trend. The probability value (p -value) is computed and then compared to the chosen significance level $\alpha = 0.05$. If the computed probability value (p value) $\leq \alpha$ ($\alpha = 0.05$), the trend is significant at 95% confident level. The

Table 2. List of Utilized climate indices (endorsed by the ETCCDI).

ID	Index name	Definitions	Units
SDII	Simple daily intensity	Total precipitation divided by the number of wet days (PRCP ≥ 1 mm)	mm/day
R10mm	Number of heavy precipitation days	Number of days when PRCP ≥ 10 mm/year	days
R20mm	Number of very heavy precipitation days	Number of days when PRCP ≥ 20 mm/year	days
Rx1day	Maximum consecutive 1-day precipitation	Maximum consecutive 1-day precipitation per year	mm
Rx5day	Maximum consecutive 5-day precipitation	Maximum consecutive 5-day precipitation per year	mm
R95p	Very wet days precipitation	Annual precipitation from days $> 95^{\text{th}}$ percentile	mm
CDD	Consecutive dry days	Maximum number of consecutive days with daily precipitation < 1 mm/year	days
CWD	Consecutive wet days	Maximum number of consecutive days with daily precipitation ≥ 1 mm/year	days

non-parametric estimation of Sen's slope determines the trend magnitude over time through a nonlinear method.

2.3.3. Correlation

For assessing the influences on variability in precipitation extremes trends, we examine correlation. Changes in pressure or temperature occurring over the different oceans affect climate variability thus climate indices and oceanic indices were used. SST based indices are computed from Extended Reconstructed SSTv5 (ERSSTv5) provided by NOAA with a horizontal resolution of $2^\circ \times 2^\circ$ during 1981-2019 (Huang et al., 2017), by referring to the climatological anomalies of the period of 1981-2010. The Niño 3.4 index stands for ENSO and which is the average SST anomalies over east-central Tropical Pacific SST (5°S - 5°N and 170° - 120°W) (Glantz & Ramirez, 2020), The IOD is represented with the dipole mode index (DMI) which is the difference of mean SST anomalies between the western (50°E - 70°E and 10°S - 10°N) and the South Eastern (90°E - 110°E and 10°S - 0°N) Equatorial Indian Ocean (Zheng et al., 2013). The annual mean change of remote indices exhibited distinct patterns and formed the foundation for interpreting their connection with extreme indices.

$$r = \frac{n(\sum xy) - (\sum x)(\sum y)}{\sqrt{[n\sum x^2 - (\sum x)^2][n\sum y^2 - (\sum y)^2]}} \quad (1)$$

where: r = Pearson Coefficient, n = number of observations for both the observational precipitation data and SSTs, $\sum xy$ = sum of for both the observational precipitation data and SSTs, $\sum x$ = sum of x observational precipitation data and $\sum y$ = sum of y SSTs.

The Pearson correlation coefficient r in expression (1) is values $-1 \leq r \leq 1$, Positive and negative trends are indicated by $r > 0$ and $r < 0$, respectively, thus the larger $|r|$, the closer the correlation between extreme indices and remote indices.

3. Results

3.1. Trend (Magnitude/Direction) and Its Significance

This study examined both magnitude and direction of trends by quantifying the linear changes expected in the variable over unit of time and indicating the variable's relationship with time, whether positive or negative.

The presented **Figure 2** illustrates the linear trends in precipitation extremes across Africa from 1981 to 2019, derived from regression coefficients of extreme indices on time. Noteworthy trends include a significant declining pattern in CWD over western, Central and northern Africa, with a rate of 0.0 - 0.15. This decreasing becomes more significant, ranging from 0.15 to 0.30, along the coasts of Nigeria and Cameroon (**Figure 2(a)**). Increasing of rate ranging 0.0 - 0.15 was observed for East Africa in Ethiopia and for South Africa in Botswana and South Africa country. Conversely, CDD exhibit a marginal decrease across central

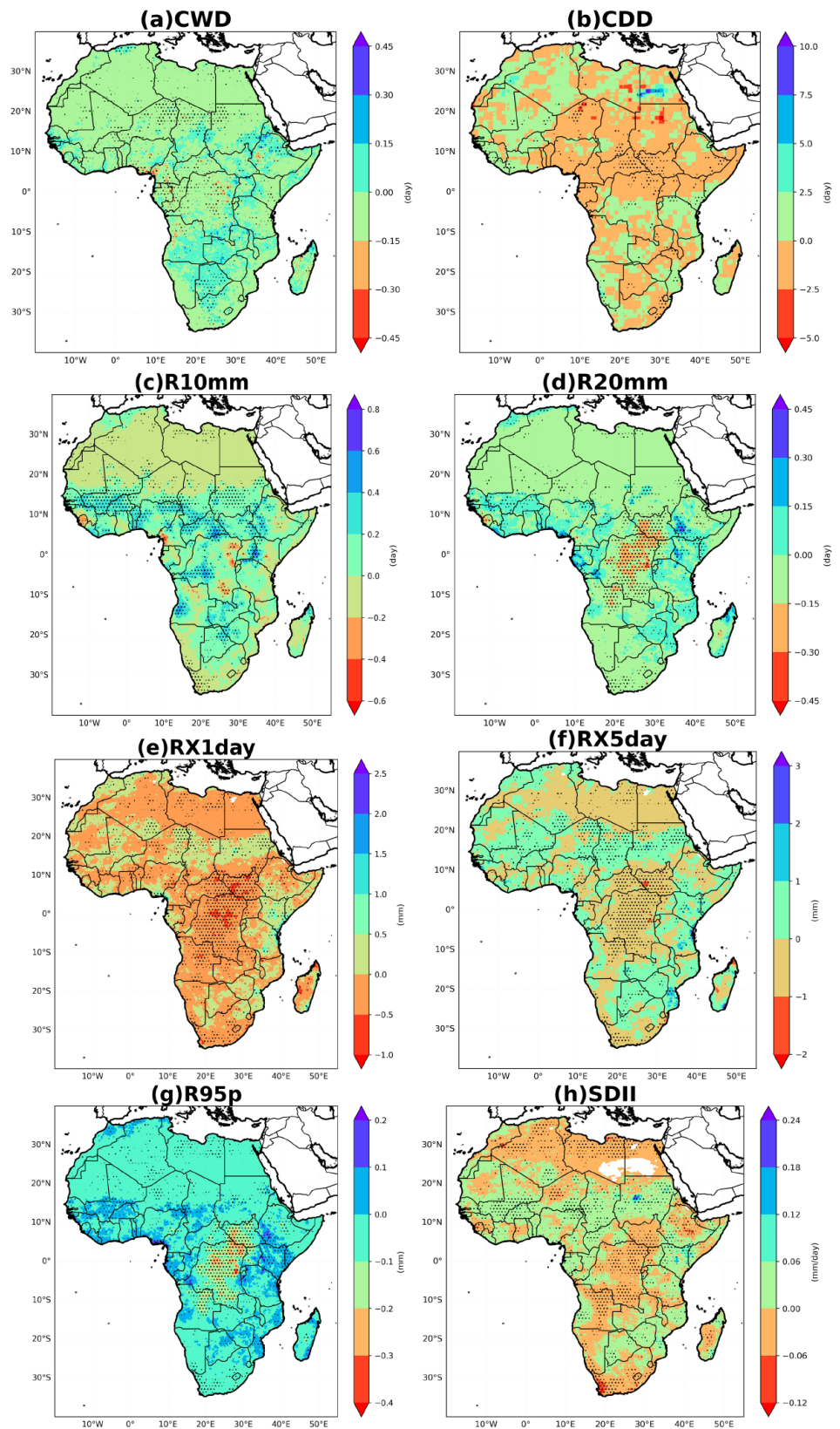


Figure 2. Spatial distributions of the linear trends of CWD, CDD, R10mm, R20mm, RX1day, RX5day, R95p and SDII over Africa during 1981-2019. Dotted areas are significant at the 95% confidence level.

Africa in DRC and Central Africa Republic, East Africa in Sudan, Ethiopia and part of Uganda, Sahara in Niger and east part of South Africa country. A tendency of upward trend is noticed in North Africa and South Africa, while a significant upward trend is observed in West Africa, specifically in Sierra Leone and Liberia, as well as in the northern part of Tanzania in East Africa (**Figure 2(b)**).

The trend for the number of heavy precipitation days with precipitation exceeding 10mm (R10mm) shows an increase of 0 - 0.6 over Western, Central, and Eastern Africa, as well as parts of Southern Africa. However, R10mm slightly decreases over various part of Northern Africa and East part of South Africa region at rate of (0 - 0.2), with a more significant decline (0.2 - 0.4) observed over Sierra Leone and the coastal areas of Cameroon (**Figure 2(c)**). Analysis of R20mm trends revealed a slight increase in East Africa and portions of Western, a marginal decrease in Sahara and Southern Africa (at a magnitude rate of 0 - 0.15), and a substantial decline (0.15 - 0.30) in the middle part of Africa, including the DRC and South Sudan (**Figure 2(d)**). The maximum 1-day precipitation (RX1day) generally decreases across the entire region (at a rate of 0 - 0.5), but showed a slight increase within the Sahara region (0 - 0.5) and a portion of Eastern Africa (0.5 - 1.0) (**Figure 2(e)**). Conversely, the 5-day maximum precipitation (RX5day) demonstrates a widespread increase, particularly pronounced in the Sahara region, Eastern Africa, and Southern Africa about magnitude rate of 1.0. However, it significantly decreases over Central Africa, Northern Africa, and the seaside areas of South Africa at rate of 0.0 - 1.0 (**Figure 2(f)**). Regarding the percentage of precipitation due to the heaviest events (R95p), an upward trend is observed throughout the West Africa and East Africa region, with substantial trends exceeding 0.1. A significant decline is noted in central Africa (at a rate exceeding -0.3), while a slight decrease is observed in the Sahel region and southern part of South Africa country (**Figure 2(g)**). The Standardized Precipitation Intensity Index (SDII) generally decreases across the majority regions of Africa with significant decline trend in central and North Africa at rate of 0 - 0.06 and 0.06 - 0.12 to the east coastal areas of South Africa country. However, a slight increase in western Africa, East Africa in Kenya, Sahara in Chad and Sudan and west part of South Africa (at magnitude rate of 0 - 0.06) (**Figure 2(h)**). Overall, the analyses revealed diverse and region-specific trends in extremes across the African continent during the specified period.

The analysis of standardized anomalies time series for various extreme precipitation indices provides valuable insights into the trend characteristics, variability and significance of these indices over the specified period. No significant decreasing trend is observed for CWD (p -value > 0.05), and the negative slope indicates a non-significant decline (**Figure 3(a)**). A significant downward trend is identified for CDD (p -value = 0.024 < 0.05), with a negative slope of -0.003 (**Figure 3(b)**). This implies a notable decline in the number of the dry spell lengths over the analyzed period for Africa. R10mm exhibits a significant downward trend (p -value = 0.013) with a positive slope of 0.02 (**Figure 3(c)**). This suggests

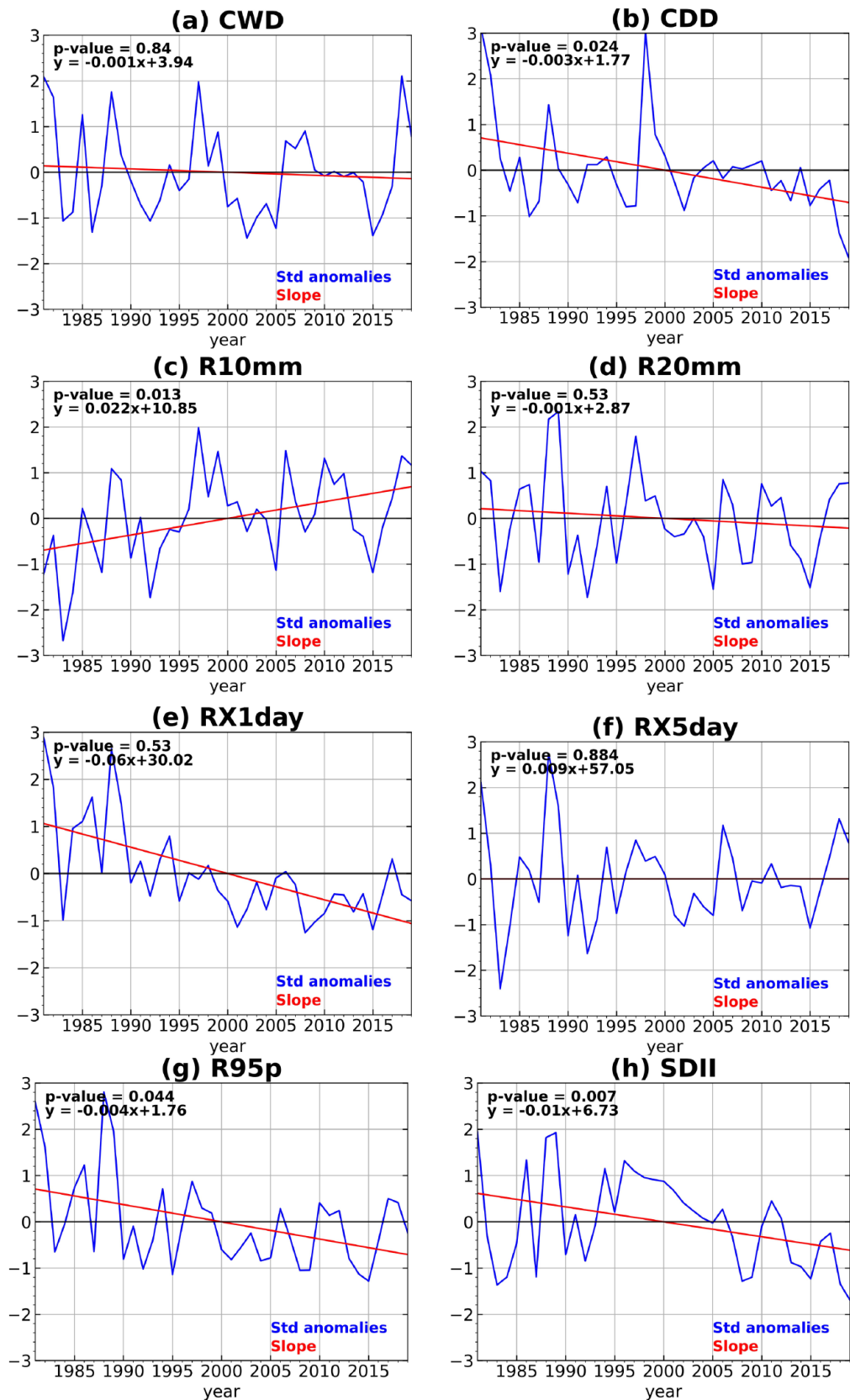


Figure 3. Standardized anomalies time series of R10mm, R20mm, CWD, CDW, R95p, SDII, RX5day and RX1day over Africa (1981-2019).

a notable rise in the frequency of heavy precipitation events. R20mm shows no significant trend (p -value = 0.52), and the negative slope of -0.001 indicates a non-significant decline in the number of days with very heavy precipitation (**Figure 3(d)**). A significant declining trend is observed for RX1day (p -value = $0.0001 \ll 0.05$), with a notable negative slope of -0.06 (**Figure 3(e)**). This indicates a substantial decline in the maximum consecutive 1-day precipitation events. No significant trend is detected for RX5day (p -value = $0.884 \gg 0.05$), and the slope strongly tends to 0 (**Figure 3(f)**). This suggests a lack of a clear trend in the maximum consecutive 5-day precipitation events. R95p shows a significant decreasing trend (p -value = 0.044) with a negative slope of -0.004 (**Figure 3(g)**). This implies a decrease in the contribution of heavy precipitation events to total precipitation. SDII exhibits a strong decreasing trend (p -value = 0.007) with a negative slope of -0.01 (**Figure 3(h)**). This suggests a notable decrease in the strength of precipitation occurrences

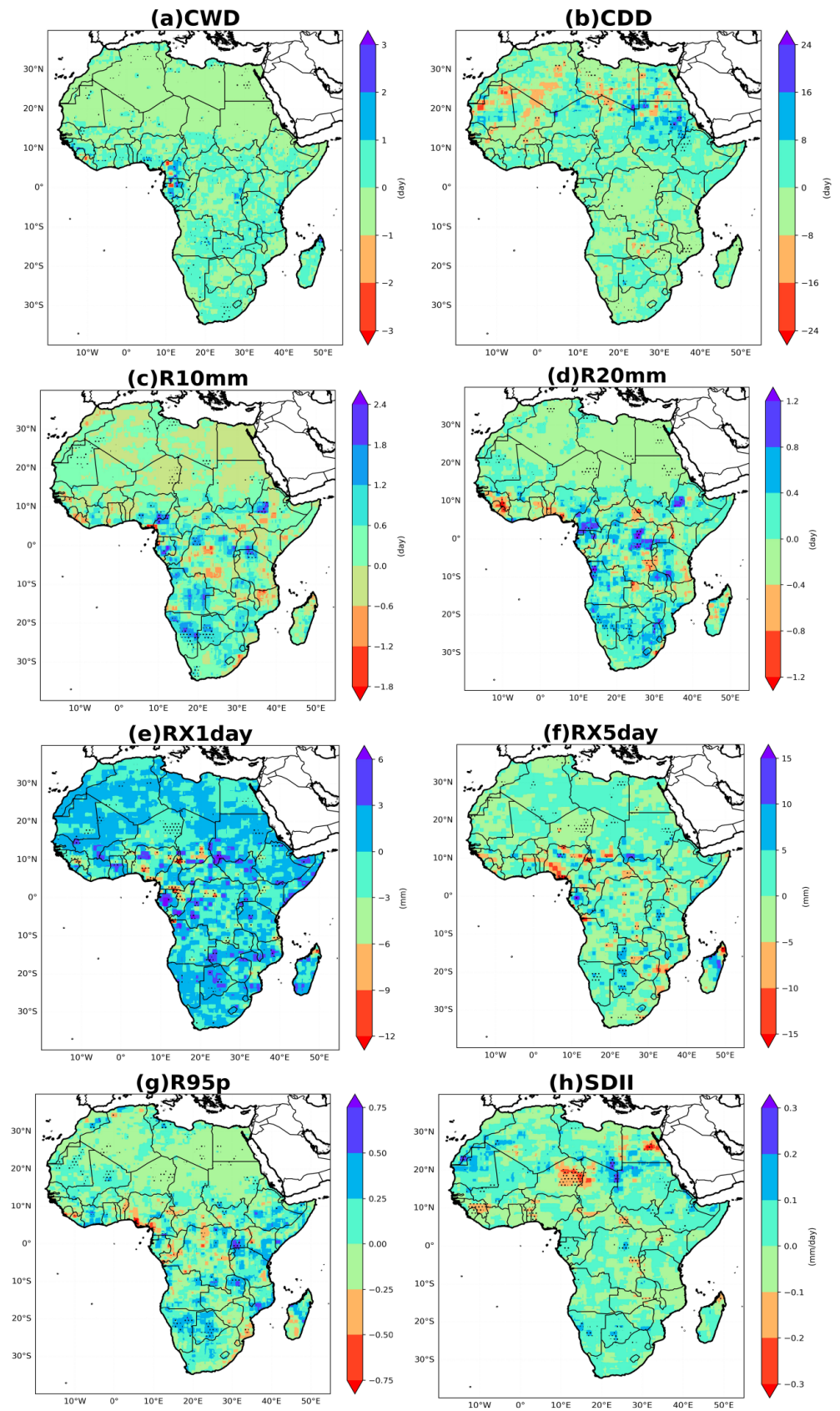
3.2. Projected Future Changes in Extreme Precipitations

Projections being part of broader climate change assessments which highlight the potential impact on local and global hydrological systems were examined in terms of extreme events in order to detect their development in the near-future period, mid-term period and long-term period under SSPs scenarios. Significant continuous decreasing changes of 0.1 - 1.0 days for SSP 1 - 2.6 and 0.1 - 1.5 days for both SSP 2 - 4.5 and SSP 5 - 8.5 in the long-term period was exhibited by CWD in Sahara region (**Figure 4**). For all regions, CWD is projected to decline by relative change 0% - 8% under SSP 1 - 2.6, 4% - 9% under SSP2-4.5, 2% - 13% under SSP 3 - 7.0 and 3% - 15% under SSP 5 - 8.5 from near to long-term period (**Figure 5**) Another significant decrease of R10mm at rate of 0.1 - 0.6 days and R20mm at rate of 0.1 - 0.4 days was exhibited in Sahara under SSP 1 - 2.6 (**Figure 4**).

Spatial features of many parts of the regions of Central Africa, West Africa, East Africa, North Africa and South Africa showed prolonged increase in extreme precipitation under low forcing scenario SSP 1 - 2.6. Under medium forcing SSP 2 - 4.5 scenario, an estimate relative change increases in CDD (0% - 5%), R10mm (0% - 7%), R20mm (4% - 7%), RX1day and RX5day (5% - 10%), R95p (0% - 2%) and SDII (1% - 3%) was highlighted from near to long-term period (**Figure 5**). While a decrease of SDII (0.1 - 0.2 mm), R20mm (0.0 - 0.1 days) is expected over North Africa, Central Africa, East Africa and some parts of South Africa in the long-term period (2081 - 2100), a significant increase of CDD (0 - 8 days), RX1day (0.0 - 2.4 mm), RX5day (0.0 - 6.0 mm) and R95p (0.0 - 0.4 mm) is projected to happen in majority parts of Africa including Madagascar under SSP 2 - 4.5 scenario (**Figure 4**).

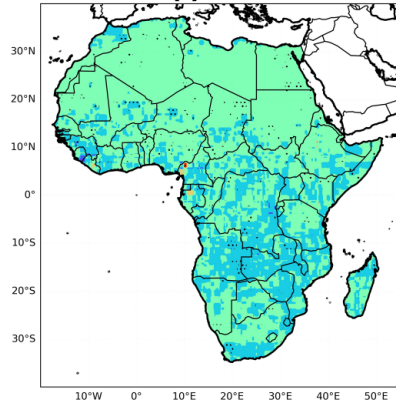
A non-significant increase of R10mm (0.0 - 1.8 days), R20mm (0.0 - 1.5 days) and CDD (0.0 - 8.0 days) in all regions of Africa under SSP 3 - 7.0 scenario was observed while CWD highlighted decrease not only Sahara region but also in Central Africa, West Africa, East Africa and South Africa for 0 - 1.5 days in

SSP1-2.6

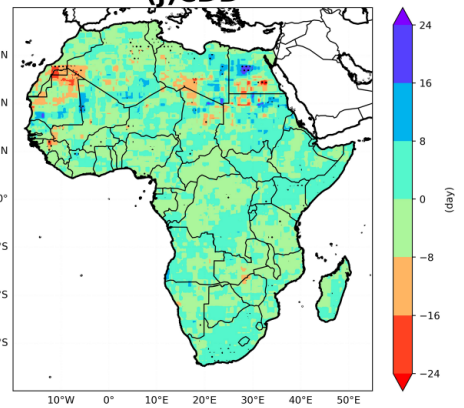


SSP2-4.5

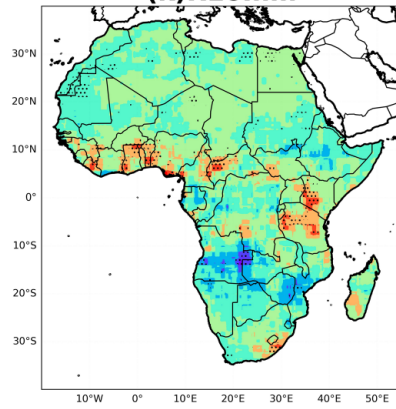
(i)CWD



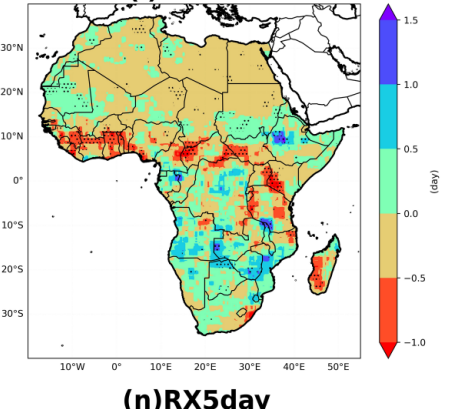
(j)CDD



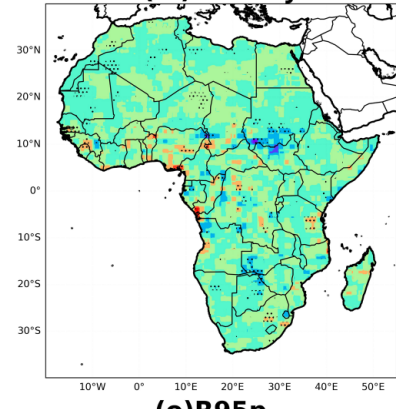
(k)R10mm



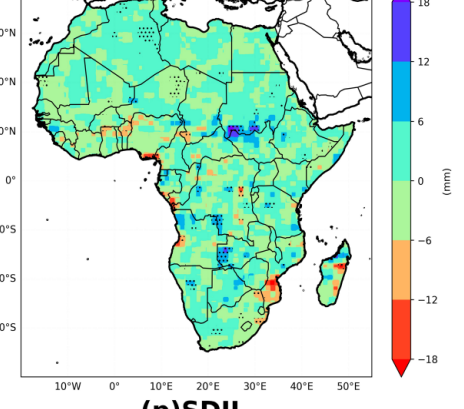
(l)R20mm



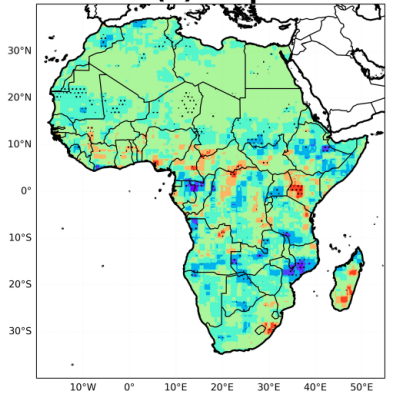
(m)RX1day



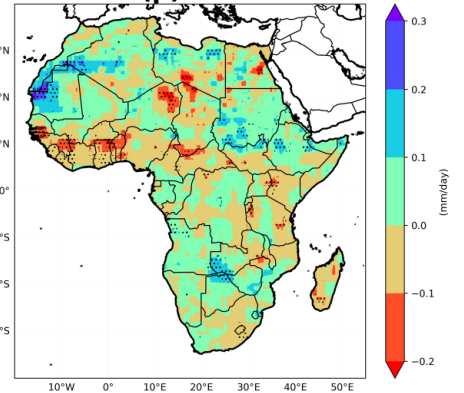
(n)RX5day



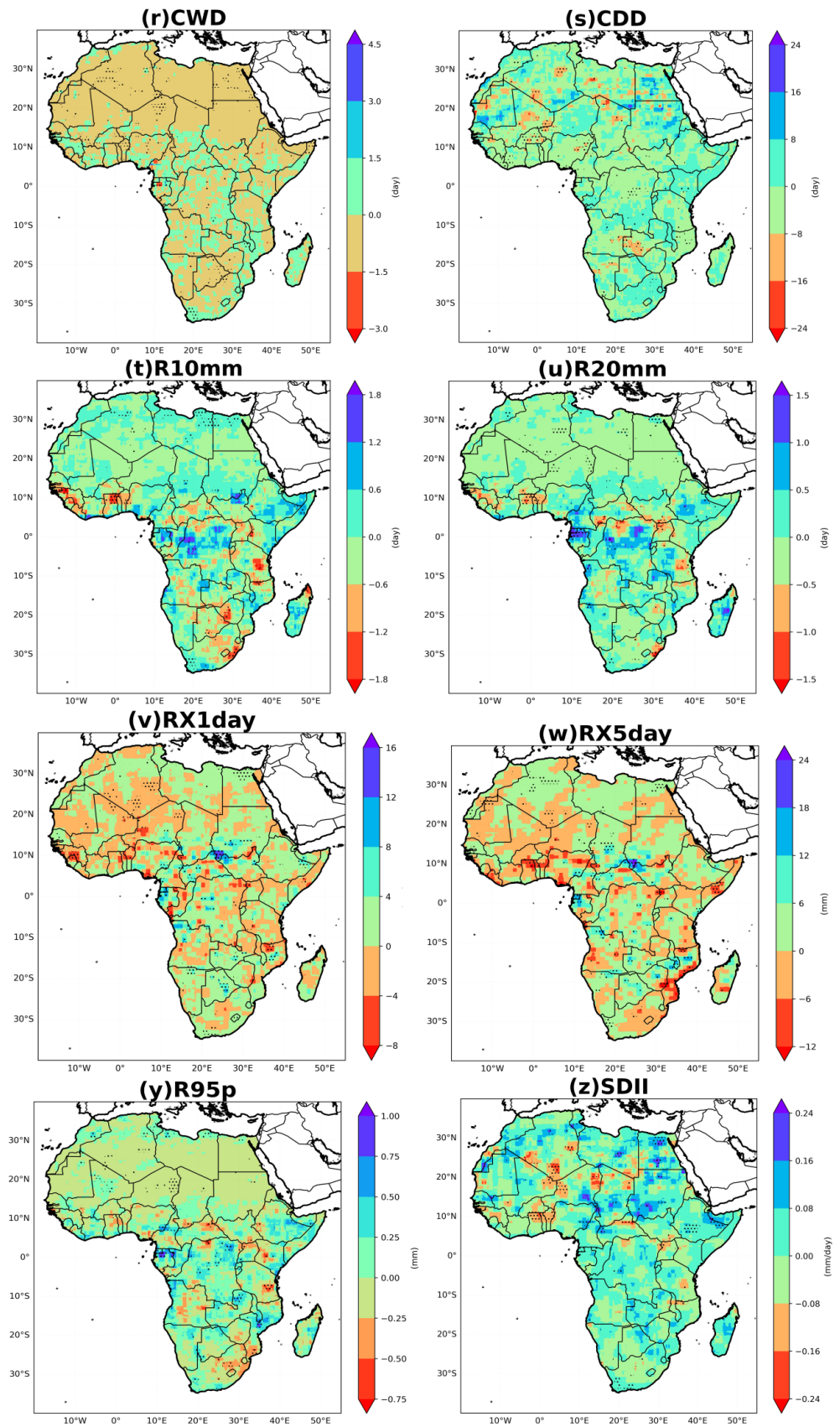
(o)R95p



(p)SDII



SSP3-7.0



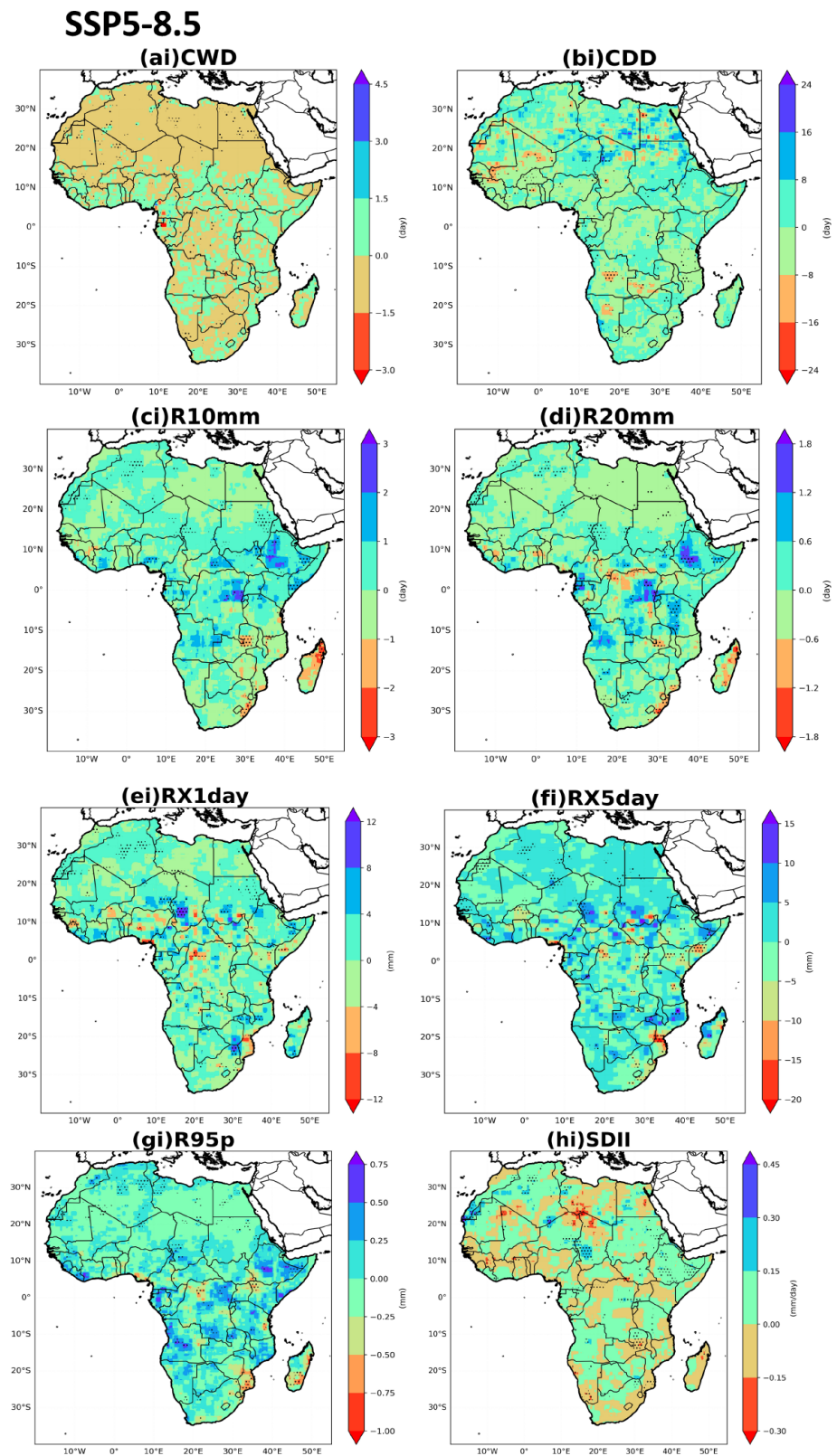


Figure 4. Projected changes in precipitation extreme indices during 2081 - 2100 under the SSP 1 - 2.6, SSP 2 - 4.5, SSP 3 - 7.0, and SSP 5 - 8.5 scenarios. The SSP 1 - 2.6 (a)-(h), SSP 2 - 4.5 (i)-(p), SSP 3 - 7.0 (r)-(z), and SSP 5 - 8.5 (ai)-(hi). Relative to base line period (1995-2014). The black dots indicate statistically significant changes at the 95% confidence level.

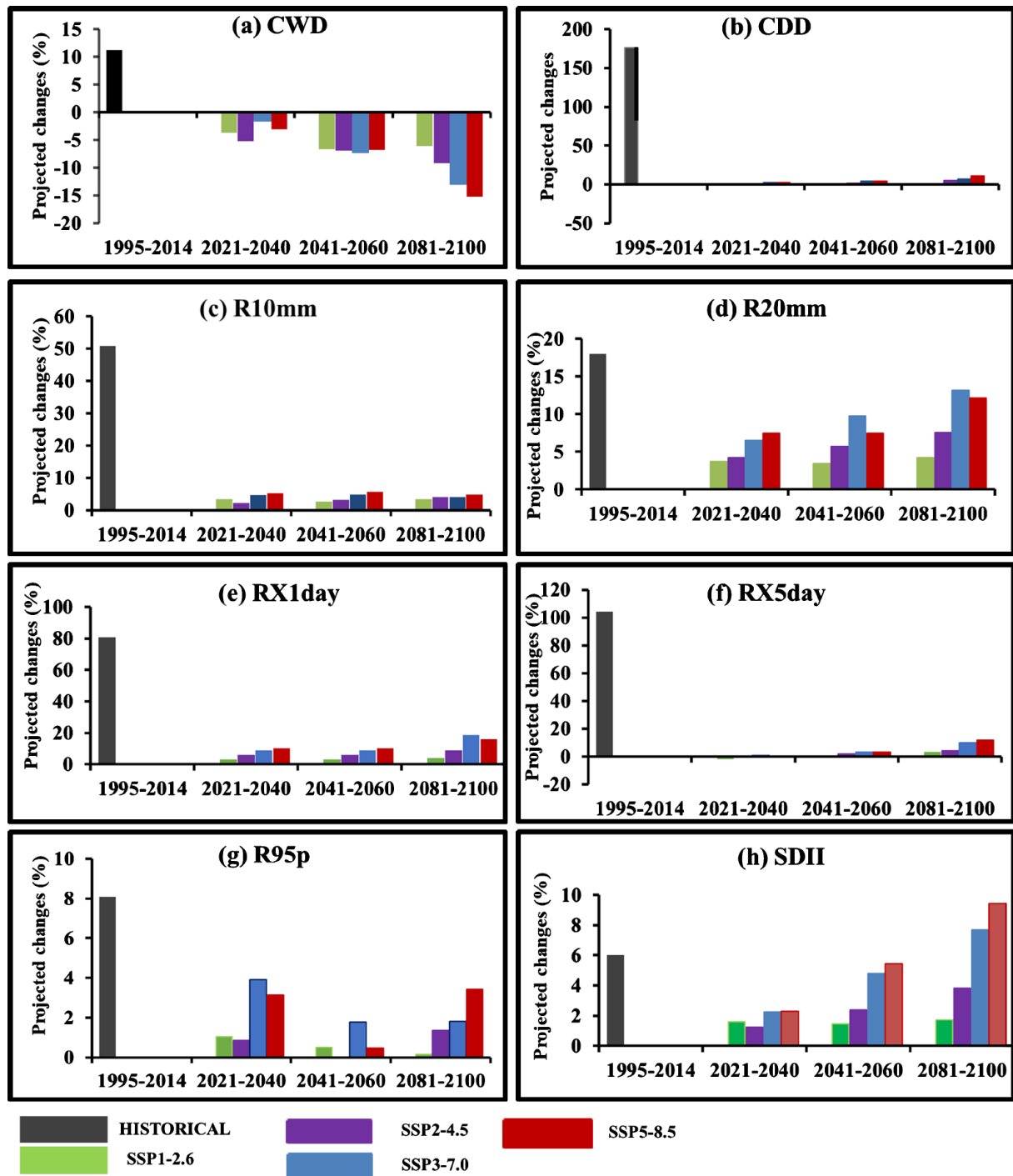


Figure 5. Projected future changes in percentage of eight extreme indices under the SSP 1 - 2.6 (Green), SSP 2 - 4.5 (Purple), SSP 3 - 7.0 (Blue) and SSP 5 - 8.5 (Red) scenarios for the near-term (2021-2040), the mid-term (2041-2060) and the far Long-term (2081-2100) relative to 1995-2014 (Black).

long-term period. In all regions under SSP 3 - 7.0, a relative change of SDII (2% - 8%), RX5day (2% - 18%) is expected from near to long-term period.

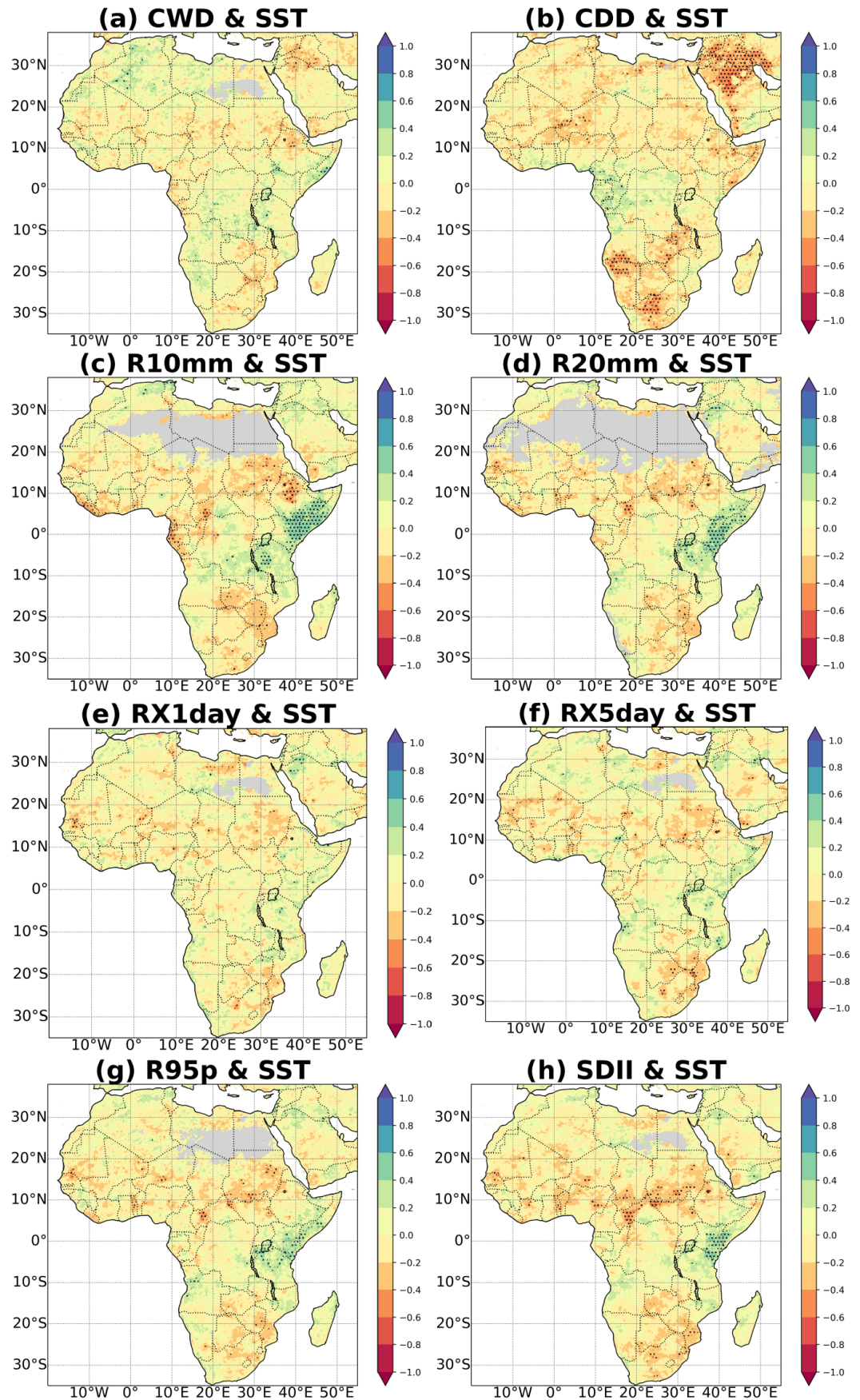
Like other scenarios, the strong force SSP 5 - 8.5 also simulate a significant upward trend in relative change of extreme rainfall in various regions of Africa, projecting a continuous increase in relative change 2% - 10% CDD, 6% - 13%

R20mm and 2% - 10% SDII (**Figure 5(b)**, **Figure 5(d)** and **Figure 5(h)**) while CWD indicate a relative change decrease of 5% - 15% from near to long-term (**Figure 5(a)**). In far future (2081-2100), days related to R10mm, R20mm, R95p and SDII are simulated to increase by 1.0 - 3.0 days, 0.6 - 1.8 days, 0.25 - 0.75 mm and 0.01 - 0.45 mm/day respectively under SSP 5 - 8.5 (**Figure 4**). This scenario shows high relative changes in majority indices in North Africa, West Africa, Central Africa, East Africa and South Africa in long-term period.

3.3. The Impacts of Oceanic Systems

Several studies have found that changes in precipitation and temperature extremes are influenced by anomalous air circulations influenced by large-scale oceanic systems such as El Niño-Southern Oscillation (ENSO), Indian Ocean Dipole (IOD) (Yu et al., 2016) and among others. To detect potential effects of oceanic systems on extremes over Africa, the correlations between detrended climate indices and indices of oceanic systems have been examined and analyzed in this study.

Figure 6 indicates the correlation patterns of the eight precipitation indices with the oceanic system indices mainly Niño 3.4 index to present ENSO and DMI for IOD. We found in our study that CDD showed a strong negative significant correlation over southern Africa (**Figure 6(b)**). R10mm, R95p and SDII show strong negative significant correlation over south part of Sahara region (**Figure 6(c)**, **Figure 6(g)**, **Figure 6(h)**). To be noticed, R10mm, R20mm, R95p and SDII also show a strong positive significant relationship with Niño 3.4 index over Eastern Africa (**Figure 6(c)**, **Figure 6(d)**, **Figure 6(g)** and **Figure 6(h)**). Precipitation extremes in East African region were also strongly influenced by IOD, as all used extreme indices showed positive correlation with IOD which was positively significant in CWD, R10mm, and R20mm (**Figure 6(i)**, **Figure 6(k)**, **Figure 6(l)**). In the same context in South Africa region, R95p, SDII, RX1day, RX5day and R20mm manifested positive significant correlation with IOD and a significant negative correlation of CDD with Niño 3.4 in the same region. West Africa region shows a negative correlation between Climate indices and Niño 3.4 index for most parts of the region only R10mm and SDII showed significant negative correlation with Niño 3.4 index in West Africa region. Contrarily, in West Africa there is positive correlation with IOD although it is not significant for all eight indices used in the study. CDD, R95p and RX5day show a weakly positive significant correlation with IOD in Sahel region especially in Soudan. RX5day and SDII indicate a weakly positive significant correlation with IOD in southern part of Algeria. To be noticed, indices (R10mm, R20mm and R95p) did not show any correlation either with Niño 3.4 index or IOD in Sahara region (**Figure 6(c)**, **Figure 6(d)**, **Figure 6(g)**, **Figure 6(k)**, **Figure 6(l)**, **Figure 6(o)**). Considering the Central African region, positive significant correlation of CWD in DRC (**Figure 6(i)**) and R10mm in Republic of Congo and Cameroun (**Figure 6(k)**), negative significant correlation of CDD was detected for IOD in



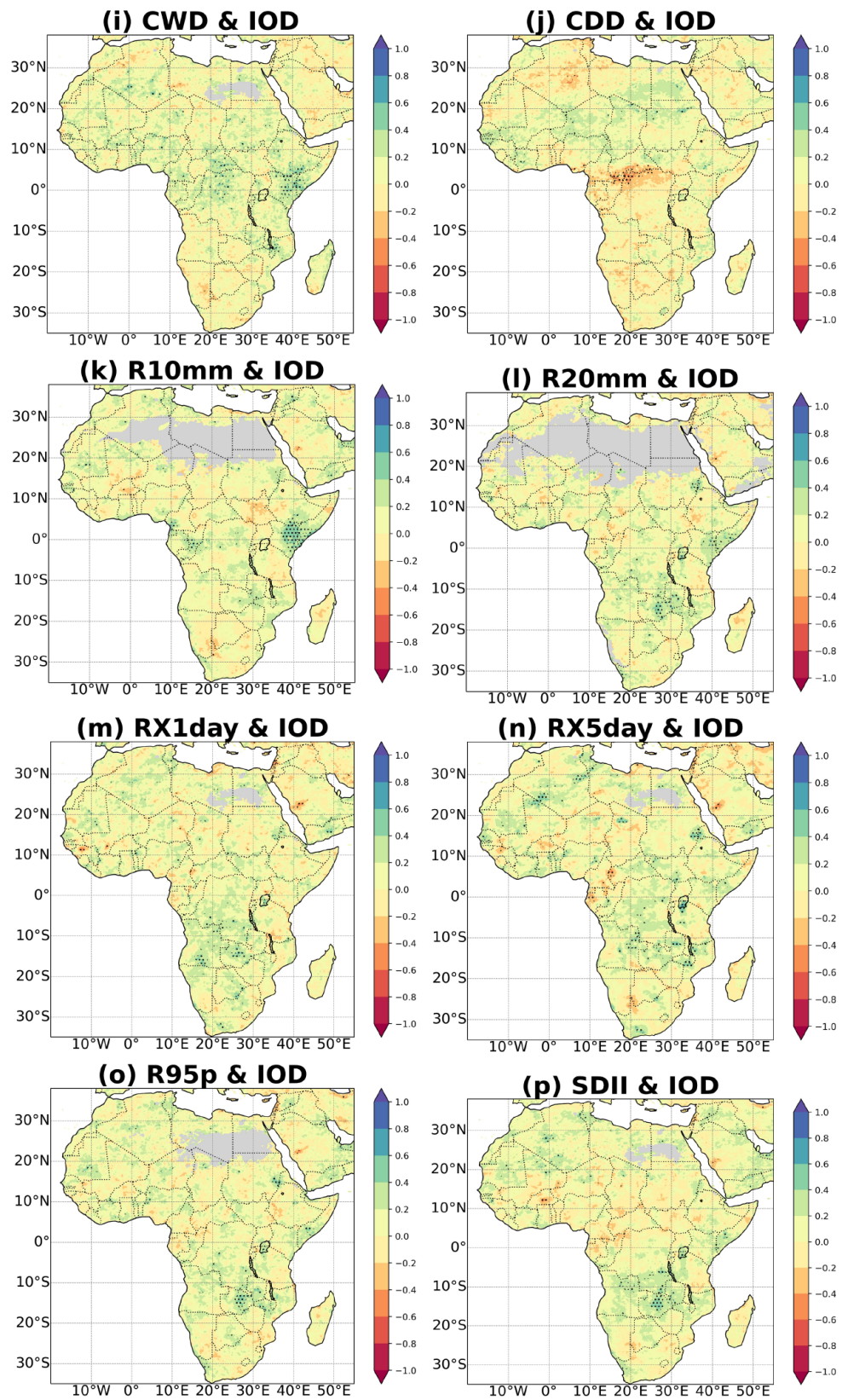


Figure 6. Correlation maps of the precipitation extreme indices with Niño-3.4 index (a)-(h) and with IOD index (i)-(p) over Africa (1981-2019). The green (red) shades denote positive (negative) correlations. Dotted regions are significant at the 0.05 significance level.

Central African Republic and DRC (**Figure 6(j)**). Central Africa precipitation is also influenced by Niño 3.4 as R10mm, SDII and R95p indices are significantly negative correlated to Niño 3.4 index specifically in Central African Republic (**Figure 6(c)**, **Figure 6(g)**, **Figure 6(h)**).

4. Discussion

The trend analyses of extreme indices over Africa from 1981 to 2019 indicate significant regional trends and fluctuations in precipitation extremes across Africa. The significance of extreme precipitation trends in certain regions of Africa is noted to be of serious concern for the future water management and agricultural practices. The areas of North Africa in general, Sahara region, Central Africa in DRC, South- Soudan and Central African Republic, west part of South Africa in Namibia and South Africa country show a tendency toward decreased extreme precipitation as shown in spatial distribution trend of extreme indices except in R10mm (**Figure 2(c)**) where it is increasing in Central Africa region. Whereas West Africa, East part of South Africa in Mozambique, Zimbabwe, Malawi and Zambia and East Africa exhibit an inclination toward increased extreme precipitation (**Figure 2**).

In East Africa region, the indices (SDII, RX1day, RX5day, R95p, CWD, and R20mm) showed a significant increasing trends, results consistent to the findings of (Palmer et al., 2023; Wainwright et al., 2021) that the warming caused by greenhouse gases leads to a rise in atmospheric moisture and its convergence amplifying wet seasons, resulting in more severe extremes of wet conditions. Increase of CWD combining with decrease of CDD indicating wetter conditions in East Africa region (Ogega et al., 2020; Ojara et al., 2021). (IPCC Working Group I et al., 2013) suggested that the shift in climate indicates regions that were previously dry will experience increased aridity, while wet areas will become even more saturated than they were in the past.

In West Africa region, CWD showed a significant decreasing trend, R10mm and R20mm have positive significant trend. The negative trend in CWD was directly associated with a southward increase in R10mm and R20mm West Africa. Similar to findings in (Quenum et al., 2021), identified a rise in R10mm and R20mm over mountainous areas and the ocean boundary. Variability of CWD and CDD could result in uneven temporal rainfall distributions. The significant decrease in CWD, RX1day and RX5day (**Figure 2**) is potentially impacting hydrological sector in West Africa region. Again the significant decreasing trend in CWD and significant increasing trends in RX5day, R95p and SDII especially in Mali, Burkina Faso and Nigeria might cause localized flood-like conditions in the region. (Diatta et al., 2020) has detected increasing of heavy rainfall in West Africa.

In central Africa region, the indices (SDII, RX1day, RX5day, R95p, CWD, CDD and R20mm) showed a significant decreasing trend. The past studies have associated the central Africa precipitation decrease with global warming (Shongwe

et al., 2009). Different studies indicate a rise in aerosol concentrations over tropical Africa (Kasoar, Shawki, & Voulgarakis, 2018; Tosca, Randerson, & Zender, 2013) should decline rainfall in Central Equatorial Africa. It was also found that the significant negative correlations between the AMO and rainfall during boreal autumn and summer in the Central Equatorial Africa support the northward shift of the Atlantic ITCZ as a cause of the declining rainfall in Central Africa (Diem et al., 2014). Central Africa region presents complex and high diversity in terms of vegetation cover, water resources, and topography. These diverse features largely influence the extreme precipitation regime (Fotso-Kamga et al., 2020). The pronounced drier conditions were detected over Sahara region where all frequency indices exhibit an inclination toward decreased extreme precipitation. Whoever RX5day and RX1day indicated significant increasing trends. Decrease in CWD and increase in RX5day, RX1day lead to drier conditions in Sahara. These increasing trends of RX5day and RX1day were impacted by direct impact of reduced dust over the Sahara, specifically the radiative effect, which results in approximately a 30% rise in precipitation compared to the increase attributed solely to the vegetation feedback (Pausata et al., 2020).

Further, the analysis of projected future changes of the extreme precipitation indicates that most of extreme indices decrease significantly across the Sahel region especially in Niger and Chad for all scenarios except CDD. However, (R10mm, R20mm, RX1day, R95p and SDII) indices for the SSP1-2.6 and SSP 2 - 4.5 scenarios increase significantly change trend in Sahel region especially in Mauritania. East Africa, (R10mm, R20mm, R95p and SDII) show an increasing precipitation extreme change trend in SSP 5 - 8.5, whereas SSP 1 - 2.6, SSP 2 - 4.5 and SSP 3 - 7.0 do not indicate a uniform pattern (trend) during long term period. This result of increasing trend depicted by these indices in East Africa, is similar to those found by (Ayugi et al., 2021) in future period. The significant increasing change trend in precipitation extreme is also seen in South Africa as (R10mm, R20mm, RX5day, R95p and SDII) for SSP 1 - 2.6 and SSP 2 - 4.5 scenarios in Botswana, Namibia and Zimbabwe. However, for the SSP 5 - 8.5 scenario, decreases in SDII are related with the decreases in CDD over parts of Zambia, indicating a generally a drier future in this region. Similar results were found by (Almazroui et al., 2020) that South Africa will experience a robust reduction in precipitation during the 21st century. West Africa region does not show a significant change in SSP 1 - 2.6 and SSP 5 - 8.5 scenarios. (SDII, CWD, R10mm and R20mm) indicate a significant decreasing change trend in West Africa indicating a drier future in the region. These outcomes are consistent with (Dosio et al., 2020, 2021) concluded a substantial reduction in rainfall pattern over West Africa in future. The outcomes of the study give us the right to conclude that Africa will continue to experience fluctuations in extreme weather and climate events. These findings are consistent with these of (IPCC, 2021) that as the Earth's climate continues to warm, there may be an escalation in the likelihood of intense precipitation events, leading to more frequent and severe flooding in certain regions. Conversely, some areas may experience extended periods of

drought due to shifts in precipitation patterns. High relative changes were projected to occur in SSP 3 - 7.0 and SSP 5 - 8.5 scenarios. In SSP 3 - 7.0, there is a lack of global cooperation and nations prioritize their own interests over collaborative efforts which lead to high challenges to mitigation (Kriegler et al, 2016) whereas in SSP 5 - 8.5, there is a continuation of current trends, with high population growth, significant reliance on fossil fuels and limited international cooperation on climate mitigation which leads to high greenhouse gas emissions and limited efforts to mitigate climate change (Kriegler et al, 2016). These factors are the main causes of high relative changes projected in future precipitation extremes.

The examination of correlation revealed a strong teleconnection between extreme indices and oceanic systems over Africa. Most of all climate indices used in our study show correlation with either Niño 3.4 or IOD. The correlation may be positive/negative in one region to another as it is significant or not. Extreme precipitation along the East Africa is highly linked to both Niño 3.4 and IOD. These results are similar to these of (Palmer et al., 2023; Wainwright et al., 2021) IOD does not have significant correlation with precipitation extreme in West and North Africa region. R10mm and SDII (Figure 4(c), Figure 4(h)) exhibit a strong negative correlation with Niño 3.4 in Ethiopia, Sudan and Central African Republic region. These findings show that the regions do not respond to unique climate drivers, but they have different variability in response to a set of large-scale. The dynamic nature of the influence exerted by each ocean in driving precipitation extreme over a specific region can vary over period. (CWD, R10mm, R20mm) in East Africa and (RX1day, RX5day, R95p, SDII) in South Africa show positive significant correlation with IOD. Well and good, in instances of positive IOD events, elevated SST anomalies in the western region and decreased SST anomalies in the eastern region result in a reversal of the zonal SST gradient, which impacts the weather, particularly precipitations, over the Indian Ocean and surrounding continents. In East Africa, increased precipitation is linked Dipole IOD phase (Wainwright et al., 2021). Extreme precipitation has numerous negative effects on the community, such as extensive flooding resulting in property damage and the loss of both human and livestock lives (Macleod et al., 2021). Within the South African context, there was a strong negative correlation of CDD with Niño 3.4 index and a significant positive correlation between R20mm, RX1day, RX5day, R95p and SDII precipitation indices and the IOD, as illustrated in (Figure 6). Previous researches demonstrated that the South African precipitation is influenced by SST in the Indian Ocean (Washington & Preston, 2006). Furthermore, the precipitation extreme of southern Africa is associated with Madden Julian Oscillation (MJO) (Silvério & Grimm, 2022). It has been pointed out that anomalies allied with the MJO during the austral summer in South America play a role in initiating the MJO in the Indian Ocean. This initiation is facilitated by equatorial teleconnections and extratropical wave trains operating in both hemispheres, establishing connections between South America and the Indian Ocean. The wave train traverses over the South Africa,

influencing rainfall patterns in this particular area (Grimm, 2019).

5. Conclusion

This study examined the trends and temporal fluctuations of precipitation extreme in Africa from 1981 to 2019, investigating future changes in extreme rainfall over the Africa under four SSPs scenarios using the latest GCMs of CMIP6 at the end of 21st century. The analysis also considered potential influences of trend variability from oceanic systems.

1) The trend analyses of extreme indices over Africa from 1981 to 2019 indicate significant regional trends and fluctuations in precipitation extremes across Africa. The regions of North Africa in general, Sahara, Central Africa (Central African Republic, DRC and South-Soudan), west part of South Africa (Namibia and South Africa) show a tendency toward decreased extreme precipitation as shown in spatial distribution trends of extreme indices (Figure 2), except R10mm (Figure 2(c)) where it is increasing in Central Africa region. Conversely, the regions of East Africa, East South Africa (Mozambique, Zimbabwe, Malawi and Zambia) and West Africa exhibit an inclination toward increased extreme precipitation (Figure 2). The analysis of trend noted that, indices (CWD, R95p, RX1day, RX5day, R10mm and R20mm) show significant increasing trend in West and East Africa regions; however, significant decreasing trends of CWD, RX5day and RX1day were detected in some areas of West Africa region. A substantial decreasing trend has been detected for CWD, CDD, R20mm, RX5day, RX1day, SDII and R95p in Central Africa, Sahara and North Africa regions. A similar trend was detected in South Africa region, except significant increasing trend exhibited by R10mm, RX5day and CWD in some parts of South Africa region and both RX5day and RX1day in some parts of Sahara region.

2) The overall projection changes of precipitation extreme indices indicate an increase in extreme precipitation intensity. Indices (R95p, SDII, RX5day and RX1day) are increasing in all scenarios over the end of 21st century. Similarly, changes in frequency indices, including CDD, R10mm and R20mm were projected to increase, too. CWD was projected to decline over the 21st century. The most notable increases are projected in R20mm and RX1day, with magnitudes of 13% and 19%, respectively, under the SSP 3 - 7.0 scenario. Conversely, projections suggest a decrease in CWD, with a magnitude of -15% under SSP 5 - 8.5 scenarios. The evolution of indices indicates a likelihood of more intense and frequent extreme rainfall events, posing an increased risk of floodings across Africa in the future.

3) Heavy precipitation in East Africa is strongly correlated to Niño 3.4 index and IOD with significant positive correlation, South Africa extreme precipitation was significant negatively (positively) correlated with Niño 3.4 and IOD respectively. Niño 3.4 was significantly teleconnected with Central Africa extreme Precipitation with negative correlation. The findings highlight that changes in SSTs or sea level pressure from various oceans can influence the distribution of ex-

extremes precipitation over different regions of Africa. The extent of this influence varies from one ocean to another and possibly across various zones within the identical ocean. Understanding these correlations is crucial for predicting and managing the consequences of climate variability in different African regions.

This research highlighted the fact that Africa precipitation is experiencing an increase and decrease in both frequency and intensity across various regions on the continent. This variability in trend of extreme precipitation has high impact on society. Escalation of extreme precipitation intensity leads to floodings and its rareness cause draughts. The findings of this research carry significant implications for policymaking in water resource management in the face of climate change. Given the region's susceptibility to severe climate change issues and extreme events, as the study highlighted, immediate action is required to implementing adaptation measures to mitigate these challenges, particularly in regions characterized by high climate variability. The study's relevance extends to the ongoing assessment and projection of drought and flood conditions, especially in regions deemed vulnerable to climate extremes. Moreover, the findings may inspire modelers and forecasters to give heightened attention to the potential consequences of precipitation extreme changes on the occurrence of extreme events, particularly in relation to heightened aridity or Inundation in the region. Furthermore, the study advocates for the use of other various indices, more multi-model ensembles GCMs and assessing more oceanic indices in future research for monitoring and understanding very well the complex interactions within the oceans and their influence on regional and global climate patterns. Finally the results of this study may provide valuable supplementary insights into precipitation extremes variability and trends in Africa, enriching the comprehension of the region's climate dynamics.

Acknowledgements

The first author expresses his gratitude to Rwanda Meteorological Agency (Meteo Rwanda), Nanjing University of Information Science & Technology (NUIST) and the Ministry of Commerce of China (MOFCOM) for huge support during the studies. Special thanks to CHIRPS, NOAA and ERA5 for providing data access. Great thanks for supervision and direction on this project to Mr. Jian Zhou, Mr. Shan Jiang, Ms. Runhong Xu, Mrs. Dusabe Diane and Mr. Mugiraneza Pierre Celestin.

Conflicts of Interest

The authors declare no conflicts of interest regarding the publication of this paper.

References

- Agarwal, S., Suchithra, A. S., & Gurjar, S. P. (2021). Analysis and Interpretation of Rainfall Trend Using Mann-Kendall's and Sen's Slope Method. *Indian Journal of Ecology*, *48*, 453-457.

- Akinsanola, A. A., Ongoma, V., & Kooperman, G. J. (2021). Evaluation of CMIP6 Models in Simulating the Statistics of Extreme Precipitation over Eastern Africa. *Atmospheric Research*, 254, Article 105509. <https://doi.org/10.1016/j.atmosres.2021.105509>
- Almazroui, M., Saeed, F., Saeed, S., Islam, M. N., Ismail, M., Klutse, N. A. B., & Siddiqui, M. H. (2020). Projected Change in Temperature and Precipitation Over Africa from CMIP6. *Earth Systems and Environment*, 4, 455-475. <https://doi.org/10.1007/s41748-020-00161-x>
- Aubry, T. J., Farquharson, J. I., Rowell, C. R., Watt, S. F. L., Pinel, V., Beckett, F. et al. (2022). Impact of Climate Change on Volcanic Processes: Current Understanding and Future Challenges. *Bulletin of Volcanology*, 84, Article No. 58. <https://doi.org/10.1007/s00445-022-01562-8>
- Ayugi, B., Dike, V., Ngoma, H., Babaousmail, H., Mumo, R., & Ongoma, V. (2021). Future Changes in Precipitation Extremes over East Africa Based on CMIP6 Models. *Water (Switzerland)*, 13, Article 2358. <https://doi.org/10.3390/w13172358>
- Barry, R. G., & Chorley, R. J. (n.d.). *Atmosphere, Weather and Climate*. Routledge. <https://www.taylorfrancis.com/books/mono/10.4324/9780203871027/atmosphere-weather-climate-roger-barry-richard-chorley>
- Brohan, P., Kennedy, J. J., Harris, I., Tett, S. F. B., & Jones, P. D. (2006). Uncertainty Estimates in Regional and Global Observed Temperature Changes: A New Data Set from 1850. *Journal of Geophysical Research Atmospheres*, 111, D12106. <https://doi.org/10.1029/2005JD006548>
- Climate Bulletin (2021). *Changing the Reference Period from 1981-2020 to 1991-2020 for the C3S Climate Bulletin*.
- Danso, D. K., Anquetin, S., Diedhiou, A., Lavaysse, C., Hingray, B., Raynaud, D., & Ko-bea, A. T. (2022). A CMIP6 Assessment of the Potential Climate Change Impacts on Solar Photovoltaic Energy and Its Atmospheric Drivers in West Africa. *Environmental Research Letters*, 17, Article 44016. <https://doi.org/10.1088/1748-9326/ac5a67>
- Dembele, M., Schaefli, B., & Van De Giesen, N. (2020). Suitability of 17 Gridded Rainfall and Temperature Datasets for Large-Scale Hydrological Modelling in West Africa. *Hydrology and Earth System Sciences*, 24, 5379-5406. <https://doi.org/10.5194/hess-24-5379-2020>
- Diatta, S., Diedhiou, C. W., Dione, D. M., & Sambou, S. (2020). Spatial Variation and Trend of Extreme Precipitation in West Africa and Teleconnections with Remote Indices. *Atmosphere*, 11, Article 999. <https://doi.org/10.3390/atmos11090999>
- Diem, J. E., Ryan, S. J., Hartter, J., & Palace, M. W. (2014). Satellite-Based Rainfall Data Reveal a Recent Drying Trend in Central Equatorial Africa. *Climatic Change*, 126, 263-272. <https://doi.org/10.1007/s10584-014-1217-x>
- Donat, M. G., Alexander, L. V., Yang, H., Durre, I., Vose, R., Dunn, R. J. H. et al. (2013). Updated Analyses of Temperature and Precipitation Extreme Indices since the Beginning of the Twentieth Century: The HadEX2 Dataset. *Journal of Geophysical Research Atmospheres*, 118, 2098-2118. <https://doi.org/10.1002/jgrd.50150>
- Dosio, A., Jury, M. W., Almazroui, M., Ashfaq, M., Diallo, I., Engelbrecht, F. A. et al. (2021). Projected Future Daily Characteristics of African Precipitation Based on Global (CMIP5, CMIP6) and Regional (CORDEX, CORDEX-CORE) Climate Models. *Climate Dynamics*, 57, 3135-3158. <https://doi.org/10.1007/s00382-021-05859-w>
- Dosio, A., Turner, A. G., Tamoffo, A. T., Sylla, M. B., Lennard, C., Jones, R. G. et al. (2020). A Tale of Two Futures: Contrasting Scenarios of Future Precipitation for West Africa from an Ensemble of Regional Climate Models. *Environmental Research Letters*, 15, Article 064007. <https://doi.org/10.1088/1748-9326/ab7fde>

- Fan, Y., Li, J., Zhu, S., Li, H., & Zhou, B. (2022). Trends and Variabilities of Precipitation and Temperature Extremes over Southeast Asia during 1981-2017. *Meteorology and Atmospheric Physics*, 134, Article No. 78. <https://doi.org/10.1007/s00703-022-00913-6>
- Fotso-Kamga, G., Fotso-Nguemo, T. C., Diallo, I., Yepdo, Z. D., Pokam, W. M., Vondou, D. A., & Lenouo, A. (2020). An Evaluation of COSMO-CLM Regional Climate Model in Simulating Precipitation over Central Africa. *International Journal of Climatology*, 40, 2891-2912. <https://doi.org/10.1002/joc.6372>
- Funk, C., Peterson, P., Landsfeld, M., Pedreros, D., Verdin, J., Shukla, S. et al. (2015). The Climate Hazards Infrared Precipitation with Stations—A New Environmental Record for Monitoring Extremes. *Scientific Data*, 2, Article No. 150066. <https://doi.org/10.1038/sdata.2015.66>
- Ge, F., Zhu, S., Luo, H., Zhi, X., & Wang, H. (2021). Future Changes in Precipitation Extremes over Southeast Asia: Insights from CMIP6 Multi-Model Ensemble. *Environmental Research Letters*, 16, Article 024013. <https://doi.org/10.1088/1748-9326/abd7ad>
- Giorgi, F., Raffaele, F., & Coppola, E. (2019). The Response of Precipitation Characteristics to Global Warming from Climate Projections. *Earth System Dynamics*, 10, 73-89. <https://doi.org/10.5194/esd-10-73-2019>
- Glantz, M. H., & Ramirez, I. J. (2020). Reviewing the Oceanic Niño Index (ONI) to Enhance Societal Readiness for El Niño's Impacts. *International Journal of Disaster Risk Science*, 11, 394-403. <https://doi.org/10.1007/s13753-020-00275-w>
- Grimm, A. M. (2019). Madden-Julian Oscillation Impacts on South American Summer Monsoon Season: Precipitation Anomalies, Extreme Events, Teleconnections, & Role in the MJO Cycle. *Climate Dynamics*, 53, 907-932. <https://doi.org/10.1007/s00382-019-04622-6>
- Hersbach, H., Bell, B., Berrisford, P., Hirahara, S., Horányi, A., Muñoz-Sabater, J. et al. (2020). The ERA5 Global Reanalysis. *Quarterly Journal of the Royal Meteorological Society*, 146, 1999-2049. <https://doi.org/10.1002/qj.3803>
- Huang, B., Thorne, P. W., Banzon, V. F., Boyer, T., Chepurin, G., Lawrimore, J. H. et al. (2017). Extended Reconstructed Sea Surface Temperature, Version 5 (ERSSTv5): Upgrades, Validations, and Intercomparisons. *Journal of Climate*, 30, 8179-8205. <https://doi.org/10.1175/JCLI-D-16-0836.1>
- Indeje, M., & Semazzi, F. H. M. (2000). ENSO Signals in East African Rainfall Seasons. *International Journal of Climatology*, 20, 19-46. [https://doi.org/10.1002/\(SICI\)1097-0088\(200001\)20:1<19::AID-JOC449>3.0.CO;2-0](https://doi.org/10.1002/(SICI)1097-0088(200001)20:1<19::AID-JOC449>3.0.CO;2-0)
- Intergovernmental Panel on Climate Change (IPCC) (2021). *Climate Change 2021. The Physical Science Basis Summary for Policymakers Working Group I Contribution to the Sixth Assessment Report of the Intergovernmental Panel on Climate Change*.
- Intergovernmental Panel on Climate Change (IPCC) (2022). *Climate Change 2022—Impacts, Adaptation and Vulnerability Working Group II Contribution to the Sixth Assessment Report of the Intergovernmental Panel on Climate Change*. Cambridge University Press. <https://doi.org/10.1017/9781009325844>
- IPCC Working Group I, Stocker, T. F., Qin, D., Plattner, G. K., Tignor, M., Allen, S. K., Boschung, J. et al. (2013). *IPCC, 2013: Climate Change 2013: The Physical Science Basis. Contribution of Working Group I to the Fifth Assessment Report of the Intergovernmental Panel on Climate Change*.
- Kasoar, M., Shawki, D., & Voulgarakis, A. (2018). Similar Spatial Patterns of Global Climate Response to Aerosols from Different Regions. *npj Climate and Atmospheric Science*, 1, Article No. 12. <https://doi.org/10.1038/s41612-018-0022-z>

- Kriegler, E., Edmonds, J., Hallegatte, S., Ebi, K. L., Kram, T., Riahi, K., Winkler, H., & Van Vuuren, D. P. (2016). A New Scenario Framework for Climate Change Research: The Concept of Shared Climate Policy Assumptions. In *Climate Policy: International Perspectives on Greenhouse Gases* (pp. 245-266). Apple Academic Press.
- Macleod, D., Kilavi, M., Mwangi, E., Ambani, M., Osunga, M., Robbins, J. et al. (2021). Are Kenya Meteorological Department Heavy Rainfall Advisories Useful for Forecast-Based Early Action and Early Preparedness for Flooding? *Natural Hazards and Earth System Sciences*, *21*, 261-277. <https://doi.org/10.5194/nhess-21-261-2021>
- Mann, H. B. (1945). Non-Parametric Test against Trend. *Econometrica*, *13*, 245-259. <https://doi.org/10.2307/1907187>
- Maraun, D., Shepherd, T. G., Widmann, M., Zappa, G., Walton, D., Gutiérrez, J. M., Hagemann, S. et al. (2017). Towards Process-Informed Bias Correction of Climate Change Simulations. *Nature Climate Change*, *7*, 764-773. <https://doi.org/10.1038/nclimate3418>
- Marra, F., Levizzani, V., & Cattani, E. (2022). Changes in Extreme Daily Precipitation over Africa: Insights from a Non-Asymptotic Statistical Approach. *Journal of Hydrology X*, *16*, Article 100130. <https://doi.org/10.1016/j.hydroa.2022.100130>
- McBride, C., Kruger, A., & Dyson, L. (2022). Changes in Extreme Daily Rainfall Characteristics in South Africa: 1921-2020. *Weather and Climate Extremes*, *38*, Article 100517. <https://doi.org/10.1016/j.wace.2022.100517>
- Ndabagenga, D. M., Yu, J., Mbawala, J. R., Ntigwaza, C. Y., & Juma, A. S. (2023). Climatic Indices' Analysis on Extreme Precipitation for Tanzania Synoptic Stations. *Journal of Geoscience and Environment Protection*, *11*, 182-208. <https://doi.org/10.4236/gep.2023.1112010>
- Nikulin, G., Lennard, C., Dosio, A., Kjellström, E., Chen, Y., Hansler, A. et al. (2018). The Effects of 1.5 and 2 Degrees of Global Warming on Africa in the CORDEX Ensemble. *Environmental Research Letters*, *13*, Article 065003. <https://doi.org/10.1088/1748-9326/aab1b1>
- Nwaerema, P., Diagi, B. E., Edokpa, D., & Ajiere, S. I. (2019). Population Variability and Heat Bias Prediction of Africa from 2019 to 2049: An Approach to Sustainable Continental Heat Management. *World Scientific News*, *130*, 265-285.
- O'Neill, B. C., Tebaldi, C., Van Vuuren, D. P., Eyring, V., Friedlingstein, P., Hurtt, G. et al. (2016). The Scenario Model Intercomparison Project (ScenarioMIP) for CMIP6. *Geoscientific Model Development*, *9*, 3461-3482. <https://doi.org/10.5194/gmd-9-3461-2016>
- Ogega, O. M., Koske, J., Kung'u, J. B., Scoccimarro, E., Endris, H. S., & Mistry, M. N. (2020). Heavy Precipitation Events over East Africa in a Changing Climate: Results from CORDEX RCMs. *Climate Dynamics*, *55*, 993-1009. <https://doi.org/10.1007/s00382-020-05309-z>
- Ogwang, B. A., Chen, H., Tan, G., Ongoma, V., & Ntwali, D. (2015). Diagnosis of East African Climate and the Circulation Mechanisms Associated with Extreme Wet and Dry Events: A Study Based on RegCM4. *Arabian Journal of Geosciences*, *8*, 10255-10265. <https://doi.org/10.1007/s12517-015-1949-6>
- Ojara, M. A., Lou, Y., Babausmail, H., & Wasswa, P. (2021). Trends and Zonal Variability of Extreme Rainfall Events over East Africa during 1960-2017. *Natural Hazards*, *109*, 33-61. <https://doi.org/10.1007/s11069-021-04824-4>
- Onyutha, C. (2017). On Rigorous Drought Assessment Using Daily Time Scale: Non-Stationary Frequency Analyses, Revisited Concepts, and a New Method to Yield Non-Parametric Indices. *Hydrology*, *4*, Article 48. <https://doi.org/10.3390/hydrology4040048>

- Onyutha, C. (2018). Trends and Variability in African Long-Term Precipitation. *Stochastic Environmental Research and Risk Assessment*, *32*, 2721-2739. <https://doi.org/10.1007/s00477-018-1587-0>
- Palmer, P. I., Wainwright, C. M., Dong, B., Maidment, R. I., Wheeler, K. G., Gedney, N. et al. (2023). Drivers and Impacts of Eastern African Rainfall Variability. *Nature Reviews Earth and Environment*, *4*, 254-270. <https://doi.org/10.1038/s43017-023-00397-x>
- Pausata, F. S. R., Gaetani, M., Messori, G., Berg, A., de Souza, D. M., Sage, R. F., & de Menocal, P. B. (2020). The Greening of the Sahara: Past Changes and Future Implications. *One Earth*, *2*, 235-250. <https://doi.org/10.1016/j.oneear.2020.03.002>
- Project Team ECA&D. Royal Netherlands Meteorological Institute KNMI (2021). *European Climate Assessment & Dataset (ECA&D). Algorithm Theoretical Basis Document (ATBD)* (pp. 1-53).
- Quenum, G. M. L. D., Nkrumah, F., Klutse, N. A. B., & Sylla, M. B. (2021). Spatiotemporal Changes in Temperature and Precipitation in West Africa. Part I: Analysis with the CMIP6 Historical Dataset. *Water (Switzerland)*, *13*, Article 3506. <https://doi.org/10.3390/w13243506>
- Raghavendra, A., Zhou, L., Jiang, Y., & Hua, W. (2018). Increasing Extent and Intensity of Thunderstorms Observed over the Congo Basin from 1982 to 2016. *Atmospheric Research*, *213*, 17-26. <https://doi.org/10.1016/j.atmosres.2018.05.028>
- Roberts, D. C., Africa, S., Mintenbeck, K., Craig, M. H., & Health, W. R. (2022). *Climate Change 2022: Impacts, Adaptation and Vulnerability Working Group II Contribution to the Sixth Assessment Report of the Intergovernmental Panel on Climate Change*.
- Schleussner, C. F., Lissner, T. K., Fischer, E. M., Wohland, J., Perrette, M., Golly, A. et al. (2016). Differential Climate Impacts for Policy-Relevant Limits to Global Warming: The Case of 1.5°C and 2°C. *Earth System Dynamics*, *7*, 327-351. <https://doi.org/10.5194/esd-7-327-2016>
- Shongwe, M. E., Van Oldenborgh, G. J., Van Den Hurk, B. J. J. M., De Boer, B., Coelho, C. A. S., & Van Aalst, M. K. (2009). Projected Changes in Mean and Extreme Precipitation in Africa under Global Warming. Part I: Southern Africa. *Journal of Climate*, *22*, 3819-3837. <https://doi.org/10.1175/2009JCLI2317.1>
- Sillmann, J., Kharin, V. V., Zhang, X., Zwiers, F. W., & Bronaugh, D. (2013). Climate Extremes Indices in the CMIP5 Multimodel Ensemble: Part 1. Model Evaluation in the Present Climate. *Journal of Geophysical Research Atmospheres*, *118*, 1716-1733. <https://doi.org/10.1002/jgrd.50203>
- Silvério, K. C., & Grimm, A. M. (2022). Southern African Monsoon: Intraseasonal Variability and Monsoon Indices. *Climate Dynamics*, *58*, 1193-1220. <https://doi.org/10.1007/s00382-021-05954-y>
- Stenchikov, G. (2021). The Role of Volcanic Activity in Climate and Global Changes. In T. M. Letcher (Ed.), *Climate Change* (3rd ed., pp. 607-643). Elsevier. <https://doi.org/10.1016/B978-0-12-821575-3.00029-3>
- Syamsuri, S., Sulistyowati, S., & Wibawa, I. (2019). Disparitas Pertimbangan Hakim Dalam Penetapan Dispensasi Kawin Dalam Prespektif Pencegahan Perkawinan Usia Dini Di Pengadilan Agama Kudus. *Jurnal Suara Keadilan*, *20*, 59-64. <https://doi.org/10.24176/sk.v20i1.5558>
- Tierney, J. E., Ummenhofer, C. C., & Demenocal, P. B. (2015). Past and Future Rainfall in the Horn of Africa. *Science Advances*, *1*, 1-9. <https://doi.org/10.1126/sciadv.1500682>
- Tosca, M. G., Randerson, J. T., & Zender, C. S. (2013). Global Impact of Smoke Aerosols from Landscape Fires on Climate and the Hadley Circulation. *Atmospheric Chemistry*

- and Physics*, 13, 5227-5241. <https://doi.org/10.5194/acp-13-5227-2013>
- Wadanambi, R. T., Wandana, L. S., Chathumini, K. K. G. L., Dassanayake, N. P., Preethika, D. D. P. et al. (2020). The Effects of Industrialization on Climate Change. *Journal of Research Technology and Engineering*, 1, 86-94.
- Wainwright, C. M., Finney, D. L., Kilavi, M., Black, E., & Marsham, J. H. (2021). Extreme Rainfall in East Africa, October 2019-January 2020 and Context under Future Climate Change. *Weather*, 76, 26-31. <https://doi.org/10.1002/wea.3824>
- Washington, R., & Preston, A. (2006). Extreme Wet Years over Southern Africa: Role of Indian Ocean Sea Surface Temperatures. *Journal of Geophysical Research Atmospheres*, 111, D15104. <https://doi.org/10.1029/2005JD006724>
- World Climate (2007). *Joint CCL/CLIVAR/JCOMM Expert Team on Climate Change Detection and Indices*. WCDMP-No. 64.
- Yahaya, I., Li, Z., Zhou, J., Jiang, S., Su, B., Huang, J. et al. (2024). Estimations of Potential Evapotranspiration from CMIP6 Multi-Model Ensemble over Africa. *Atmospheric Research*, 300, Article 107255. <https://doi.org/10.1016/j.atmosres.2024.107255>
- Yu, L., Zhong, S., Pei, L., Bian, X., & Heilman, W. E. (2016). Contribution of Large-Scale Circulation Anomalies to Changes in Extreme Precipitation Frequency in the United States. *Environmental Research Letters*, 11, Article 044003. <https://doi.org/10.1088/1748-9326/11/4/044003>
- Zhang, P., Ren, G., Xu, Y., Wang, X. L., Qin, Y., Sun, X., & Ren, Y. (2019). Observed Changes in Extreme Temperature over the Global Land Based on a Newly Developed Station Daily Dataset. *Journal of Climate*, 32, 8489-8509. <https://doi.org/10.1175/JCLI-D-18-0733.1>
- Zhang, X., Alexander, L., Hegerl, G., Jones, P., Tank, A., Peterson, T. et al. (2011). Indices for Monitoring Changes in Extremes Based on Daily Temperature and Precipitation Data. *Wiley Interdisciplinary Reviews: Climate Change*, 2, 851-870. <https://doi.org/10.1002/wcc.147>
- Zheng, X.-T., Xie, S.-P., Du, Y., Liu, L., Huang, G., & Liu, Q. (2013). Indian Ocean Dipole Response to Global Warming in the CMIP5 Multimodel Ensemble. *Journal of Climate*, 26, 6067-6080. <https://doi.org/10.1175/JCLI-D-12-00638.1>